

# The critical exponents of fracture precursors

A. Guarino\*, R. Scorretti\*, S. Ciliberto\* and A. Garcimartín†

\*Ecole Normale Supérieure de Lyon, 46 allée  
d'Italie, 69364 Lyon, France

†Departamento de Física, Facultad de  
Ciencias, Universidad de Navarra,  
E-31080 Pamplona, Spain.

## Abstract

The acoustic emission of fracture precursors is measured in heterogeneous materials. The statistical behaviour of these precursors is studied as a function of the load features and the geometry. We find that the time interval  $\delta t$  between events (precursors) and events energies  $\varepsilon$  are power law distributed and that the exponents of these power laws depend on the load history and on the material. In contrast, the cumulated acoustic energy  $E$  presents a critical divergency near the breaking time  $\tau$  which is  $E \sim \left(\frac{\tau-t}{\tau}\right)^{-\gamma}$ . The positive exponent  $\gamma$  is independent, within error bars, by all the experimental parameters.

**PACS:** 62.20.Mk, 05.20.-y, 81.40.Np

Heterogeneous materials are widely studied not only for their large utility in applications but also because they could give more insight to our understanding of the role of macroscopic disorder on material properties. The statistical analysis of the failure of these materials is an actual and fundamental problem which has received a lot of attention in the last decade both theoretically [1]-[18] and experimentally [19]-[24]. When an heterogeneous material is stretched its evolution toward breaking is characterized by the appearance of microcracks before their final break-up. Each microcrack produces an elastic wave which is detectable by a piezoelectric microphone. The microcracks constitute the so called precursors of fracture.

The purpose of this letter is just to describe a detailed statistical analysis of fracture precursors performed under many different experimental conditions and in several heterogeneous materials. Analysis of this kind can give very useful informations for constructing realistic statistical models of material failure. In our experiments we apply a pressure  $P$  to an heterogeneous sample until failure. The parameters that we consider are the elapsed time  $\delta t$  between two consecutive events, the acoustic energy  $\varepsilon$  released by a single microcrack and the acoustic energy cumulated since the beginning of the loading  $E$ . In this paper we discuss the statistical behavior of these parameters as a function of the load applied to the sample, the material elastic properties and the geometry.

In previous experiments it has been shown [23, 24] that if a quasi-static <sup>1</sup> constant pressure rate is imposed, that is  $P = A_p t$ , the sample breaks in a brittle way. In this case the cumulated acoustic energy  $E(t)$  ( i.e. the total energy released up to a time  $t$  by the microfractures) scales with the reduced time or pressure<sup>2</sup> in the following way:

$$E \sim \left(\frac{\tau - t}{\tau}\right)^{-\gamma} ,$$

where  $t$  is time, the critical time  $\tau$  is the time at which the sample breaks and  $\gamma = 0.27 \pm 0.05$  for all the materials we have checked. In contrast, if a constant strain rate  $u = Bt$  is imposed, a plastic fracture is observed and the released energy shows no critical behavior. We have also shown that in the case of a constant  $P$  imposed to the sample (creep test), the total energy  $E$  becomes, near failure, a function of  $t$  and scales as  $E \sim \left(\frac{\tau - t}{\tau}\right)^{-\gamma_c}$ .

---

<sup>1</sup>A load is considered quasi-static if the load rate is lower than the relaxation time of the system.

<sup>2</sup>In this case  $P$  and  $t$  are proportional.

Notably, the exponent found when a constant stress is applied is the same than the one corresponding to the case of constant stress rate [25]:  $\gamma = \gamma_c$ . In all of the processes, at constant pressure and at constant pressure rate, the actual control parameter for failure seems to be the time. The appearance of a microcrack seems to be due to a nucleation process [17, 18], and the probability of nucleation determines the lifetime  $\tau$  of the entire sample. In fact, we find that  $\tau$  is given by the equation:

$$\int_0^\tau \frac{1}{\tau_o} e^{-(\frac{P_o}{P})^4} dt = 1 \quad ,$$

where  $P$  is the pressure and  $\tau_o$  and  $P_o$  are constants, which depends on the material and on the geometry [25].

In the case of constant load rate ( $P = A_p t$  or  $u = B t$ ) the system has not a characteristic scale of energy or time: the histogram  $N(\varepsilon)$  of the released energy and the histogram  $N(\delta t)$  of the elapsed time  $\delta t$  between two consecutive events reveal power laws, i.e.  $N(\varepsilon) \sim \varepsilon^{-\beta}$  and  $N(\delta t) \sim \delta t^{-\alpha}$ . The exponents  $\alpha$ ,  $\beta$  and  $\gamma$  do not depend on the load rate  $A_p$  or  $B$  [23, 24]. In this paper we are interested in studying the exponents in different geometries and when a constant (creep test), cyclic or erratic load are imposed.

The tests are performed by monitoring the acoustic emission (AE) released before the final break-up of a sample on a high pressure chamber (HPC) machine. The sample separates two chambers and a pressure difference  $P$  is imposed between them. A sketch of the apparatus is shown in fig. 1a and 1b. We have prepared circular wood (Young modulus  $Y = 2 \cdot 10^8 N/m^2$ ) and fiberglass samples of 22 cm diameter and 4 mm thickness. The Young modulus of these materials are  $Y = 2 \cdot 10^8 N/m^2$  for wood and  $Y = 2 \cdot 10^8 N/m^2$  for fiberglass. The AE consists of ultrasound bursts (events) produced by the formation of microcracks inside the sample. For each AE event, we record the energy  $\varepsilon$  detected by the four microphones <sup>3</sup>, the place where it was originated, the time at which the event was detected and the instantaneous pressure and displacement at the center of the sample. We are able to record up to 33 events per second. The experimental apparatus is the same that has been used to obtain the previously cited results; a more detailed description of the experimental methods can be found in [23, 24].

---

<sup>3</sup>The energy is defined as the integral of the sum of the squared signals.

To check the dependence of  $\alpha$ ,  $\beta$  and  $\gamma$  on the geometry, we used a classical tensile machine, fig 1c. The force applied to the sample is slowly and constantly increased up to the final break-down of the sample. During the load we measure the applied force  $F$ , the strain, the AE produced by microcracks and the time at which the event was detected. The samples have a rectangular shape, with a length of 29 cm, a height of 20 cm and a thickness of 4 mm. More details of the experimental setup can be found in [26].

In the experiments performed with the first apparatus (HPC), power laws are obtained for the distributions of  $\epsilon$  and of  $\delta t$ . As an example of two typical distributions obtained at constant imposed pressure, we plot in fig 2a) and 2b)  $N(\delta t)$  and  $N(\delta\epsilon)$  respectively. The exponents of these power laws ( $\alpha_c$  for energies and  $\beta_c$  for times) depend on  $P$ . In fig. 2c,  $\alpha_c$  and  $\beta_c$  are plotted versus  $P$ . Note that both exponents grow with pressure. We observe that the rate of emissions increases with pressure, so that the weight of big values of  $\delta t$  decreases. This explains the fact that  $\beta_c$  grows with pressure. We have compared the histograms of energy  $\epsilon$  for several pressures, and we noticed that the number of high-energy emissions is almost the same, while the number of low-energy emissions increase with pressure, so that the exponent  $\alpha_c$  increases as well. Moreover, as the pressure increases, the exponents  $\alpha_c$  and  $\beta_c$  attain the values  $\alpha = 1.9 \pm 0.1$  and  $\beta = 1.51 \pm 0.05$  obtained in the case of a constant loading rate[24]. We imposed to the sample a cyclic and an erratic load, which are plotted as a function of time in figure 3a and 3b respectively. Power laws are obtained for the distributions of  $\epsilon$  and for  $\delta t$ . The exponents of these power laws do not depend on the load behavior; their value is the same of that at constant loading rate. These and previous results [23, 24], allows us to state that if  $\frac{dP}{dt} \neq 0$ , the histograms of the released energy  $\epsilon$  and of the time intervals  $\delta t$  do not depend on the load history. The fact that  $\alpha$  and  $\beta$  do not depend on  $\frac{dP}{dt}$  seems to be in contrast with the fact that  $\alpha_c$  and  $\beta_c$  depend on  $P$ . This result can be interpreted by considering that the microcracks formation process is not the same when  $\frac{dP}{dt} = 0$  and  $\frac{dP}{dt} \neq 0$ . In the former case, imposed constant  $P$ , the mechanism of microcrack nucleation is the dominant one and the nucleation time depend on pressure. In the other case,  $\frac{dP}{dt} \neq 0$ , the dominant mechanism is not the nucleation but the fact that, when pressure increases as a function of time, several parts of the sample may have to support a pressure larger than the local critical stress to break bonds. The fact that at high constant pressure  $\alpha_c$  and  $\beta_c$  recover

the value  $\alpha_c$  and  $\beta_c$  has a simple explanation. Indeed, in order to reach a very high pressure  $P_h$ ,  $\frac{dP}{dt}$  is different from zero for a time interval which is comparable or even larger than the time interval spent at constant pressure  $P_h$ . Thus at high constant pressure the system is close to the case  $\frac{dP}{dt} \neq 0$ .

Using the cyclic and the erratic pressure, plotted respectively in fig. 3a and 3b, we can check the dependence of  $\gamma$  on the history of the sample, i.e. on the behavior of the imposed pressure. The cumulated energy  $E$  for the cyclic and the erratic pressure, shown in fig 3a and 3b as a function of  $t$ , is plotted in log-log scale as a function of the reduced parameter  $\frac{\tau-t}{\tau}$  in fig 4a and 4b respectively. We observe that, in spite of the fluctuations due to the strong oscillations of the applied pressure, near the final break-up the energy  $E$ , as a function of  $\frac{\tau-t}{\tau}$ , is fitted by a power law with  $\gamma \simeq 0.27 \pm 0.02$ . In fig.4c),  $E$  measured when a constant pressure is applied to the sample is plotted as a function of  $\frac{\tau-t}{\tau}$ . A power law is found in this case too [25]. The exponent  $\gamma$  is, within error bars, the same in the three cases. Hence it depends neither on the applied pressure history nor on the material [23, 24, 25].

Further, experiments made with the tensile machine show that  $\gamma$  is independent on the geometry. In fact we observe that the behavior of the energy near the fracture as a function of  $(\frac{\tau-t}{\tau})$  is still a power law of exponent  $\gamma \simeq 0.27$ , as shown in figure 4d.

Considering the experimental data here presented and those already published [23, 24], we claim that, if a load is imposed to an heterogeneous material, power laws are obtained for the histograms of the released energy  $\varepsilon$  and of the time intervals  $\delta t$ . The exponents of these power laws depend on the material and, if  $\frac{dP}{dt} = 0$ , on the applied pressure  $P$ . In contrast, at imposed pressure, the behavior of the cumulated energy  $E$  near the final breaking point does not depend on the load, on the geometry and on the material [23, 24, 25]. We find that time is the control parameter of the system and that  $E \sim (\frac{\tau-t}{\tau})^{-\gamma}$ , where the critical exponent is  $\gamma = 0.27 \pm 0.05$ . These results are quite similar to those obtained with numerical simulations on a democratic bundle fiber model with thermal noise. These facts and the observed dependence of  $\tau$  on  $P$  allow us to conclude that microcrack nucleation process [17, 18] plays a fundamental role in the entire dynamics of the system. These are very useful informations in order to construct a realistic statistical model of heterogenous material failure.

## References

- [1] Kanninen M.F. and Popelar C.H., *Advanced Fracture Mechanics* (Oxford University Press, NewYork, 1985).
- [2] Lawn B., *Fracture of Brittle Solids* (Cambridge University Press, Cambridge 1993, 2nd. edition).
- [3] Herrmann H.J. and Roux S., Eds., *Statistical models for the fracture of disordered media* (North-Holland, Amsterdam, 1990).
- [4] Atkinson B. K., *Introduction to fracture mechanics*, Academic Press (1989).
- [5] Shah S. P. *Toughening Mechanisms in Quasi Brittle Materials*, Kluwer Accademic Publisher (1991).
- [6] Dieter G., *Mechanical Metallurgic*, Mc Graw Hill, (1988).
- [7] Naimark O.B. and Silberschmidt V.V., *Eur. J. Mech. A / Solids* **10** (1991) 607.
- [8] Bouchaud E., *J. Phys. Condens. Matter* **9** (1997) 4319.
- [9] Hansen A., Hinrichsen E.L. and Roux S., *Phys. Rev. Lett.* **66** (1991) 2476.
- [10] Hemmer, P.C. , Hansen A. *J. Appl. Mech.* 59 909 (1992)
- [11] Zapperi S., Vespignani A. and Stanley H.E., *Nature*, vol **338**, 658-660 (1997).
- [12] Zhou S. J., Bearzley D. M., Lomdahl P.S.and Holian B. L., *Phys. Rev. Lett.* **78** (1997) 479; Zhou S. J., Carlson A. E. and Thomson R., *Phys. Rev. Lett.* **72** (1994) 852,.
- [13] P. Bak, C. Tang, K. Wiesenfield, *Phys. Rev. Lett.* 59, 381 (1987).
- [14] De Arcangelis L. and Hermann H. J., *Phys. Rev. B* **39** (1989) 2678; De Arcangelis L., Hansen H., Herrmann H. J. and Roux S., *Phys. Rev. B* **40** (1989) 877
- [15] Sornette D. and Vanneste C., *Phys. Rev. Lett.* **68** (1992) 612.

- [16] Mogi K., *Bull. Earth Res. Inst. Tokyo* **40**, 125- (1962).
- [17] Pomeau Y., Brisure spontanée des cristaux bidimensionnel courbés, C. R. Acad. Sci. Paris , vol. **314** II, 553-556 (1992).
- [18] Gobulović L. and Feng S., Rate of microcrack nucleation, *Pys. Rev. A*, **40**, 5223-5227,10 (1991).
- [19] Stead D. and Szczepanik Z., Acoustic emission during uniaxial creep in potash. *Fifth conference on acoustic emission/ microseismic activity in geologic structures and materials*, Pennsylvania State Univ., 97-111 (1991).
- [20] Maes C. Van Moffaert A., Frederix H. and Strauven H., *Phys. Rev. B* **57** 9, 4987-4990 (1998).
- [21] D.A. Lockner, J.D. Byerlee, V. Kuksenko, A. Ponomarev, A. Sidorin, *Nature* 350, 39 (1991).
- [22] A. Petri, G. Paparo, A. Vespignani, A. Alippi, M. constantini, *Phys. Rev. Lett.* 73, 43423 (1994).
- [23] Garcimartín A., Guarino A., Bellon L. and Ciliberto S., *Phys. Rev. Lett.* **79** 17, 3202-3205 (1997).
- [24] Guarino A., Garcimartín A. and Ciliberto S., *European Physical Journal B*, 6, 13-24 (1998).
- [25] Guarino A., Garcimartín A. and Ciliberto S., Failure time and microcrack nucleation, Submitted to the Europhysics letters.
- [26] Boudet J.F., S. Ciliberto and V. Steinberg. Dynamic of crack propagation in brittle materials. *J. Phys II*, **6**, 1493-1516 (1996).

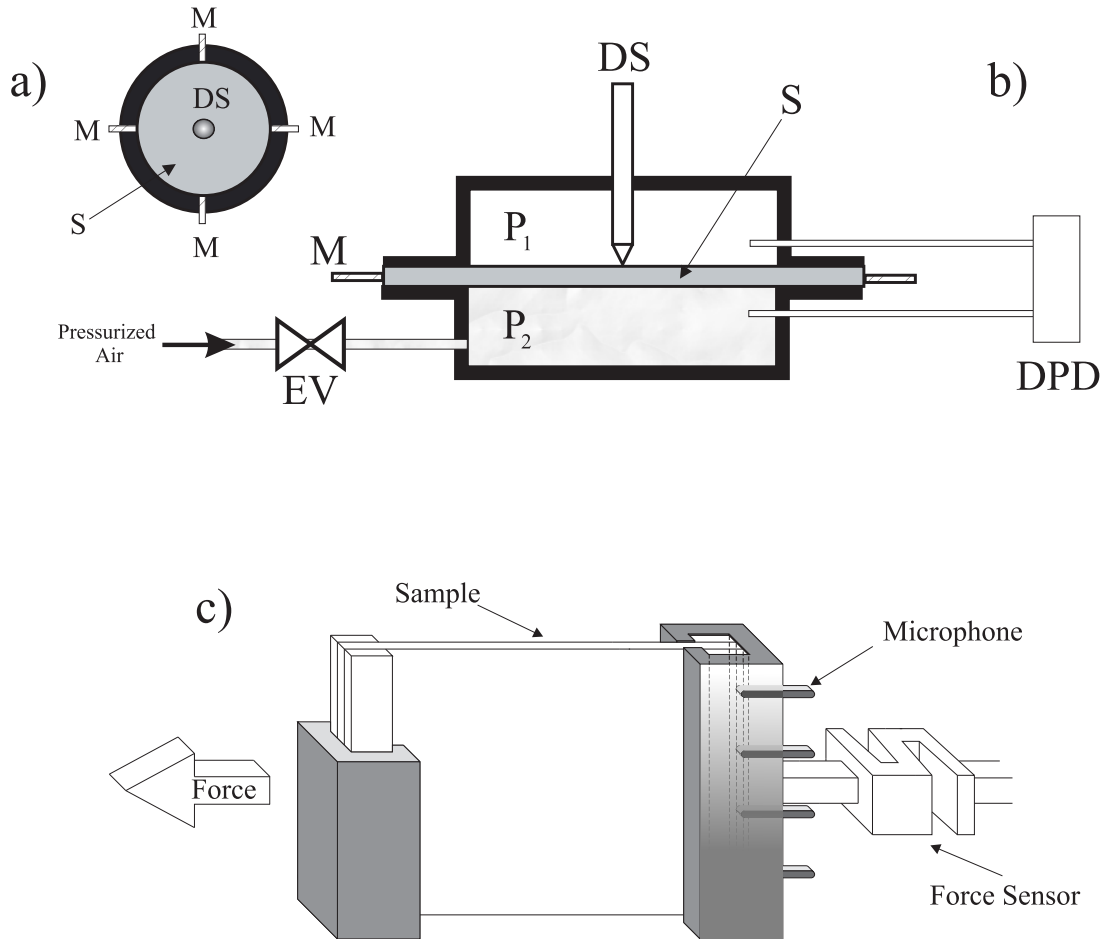


Figure 1: **a, b)** Sketch of the high pressure chamber (HPC) apparatus. S is the sample, DS is the inductive displacement sensor (which has a sensitivity of the order of  $1 \mu\text{m}$ ). M are the four wide-band piezoelectric microphones.  $P=P_1-P_2$  is the pressure supported by the sample. P is measured by a differential pressure sensor (sensitivity 0.002 atm) that is not represented here. EV is the electronic valve which controls P via the feedback control system Ctrl. HPR is the high-pressure air reservoir. **c)** Sketch of the tensile machine. An uniaxial force, which is measured by a piezoresistive sensor, is applied to the sample by a stepping motor. Four wide-band piezoelectric microphones measure the acoustic emissions emitted by the sample. Experiments have been done using rectangular (20 x 29 cm) wood samples of 4 mm thickness. The whole apparatus is surrounded by a Faraday screen.

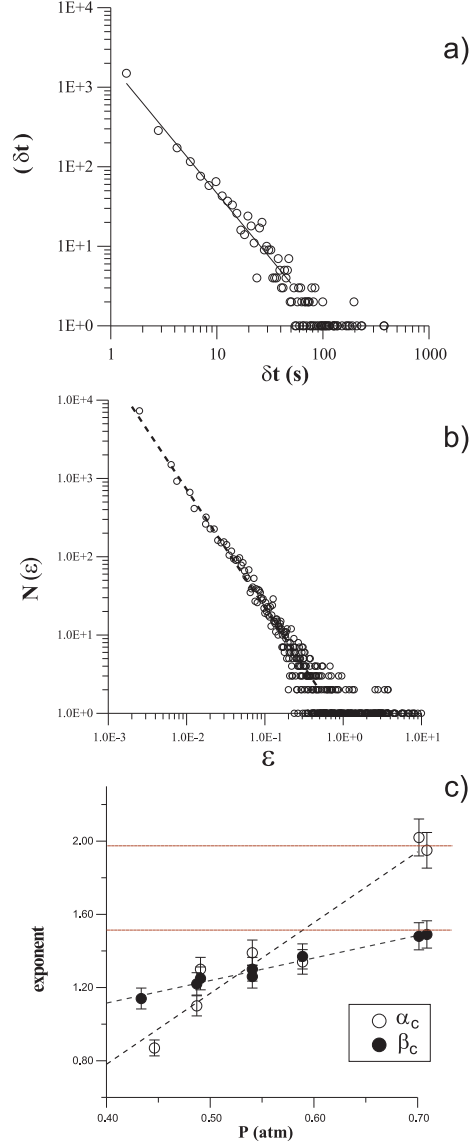


Figure 2: **a,b)** Two typical time  $\delta t$  and energy  $\varepsilon$  distributions obtained at imposed constant pressure ( $P = 0.56 \text{ atm}$ ). **c)** The exponents  $\alpha_c$  (empty circles) and  $\beta_c$  (black points), plotted as a function of the value of the imposed constant pressure. Note that as the pressure increases, the values of the exponents tend to those obtained in the case of constant pressure rate. The error bars represent the statistical uncertainty.

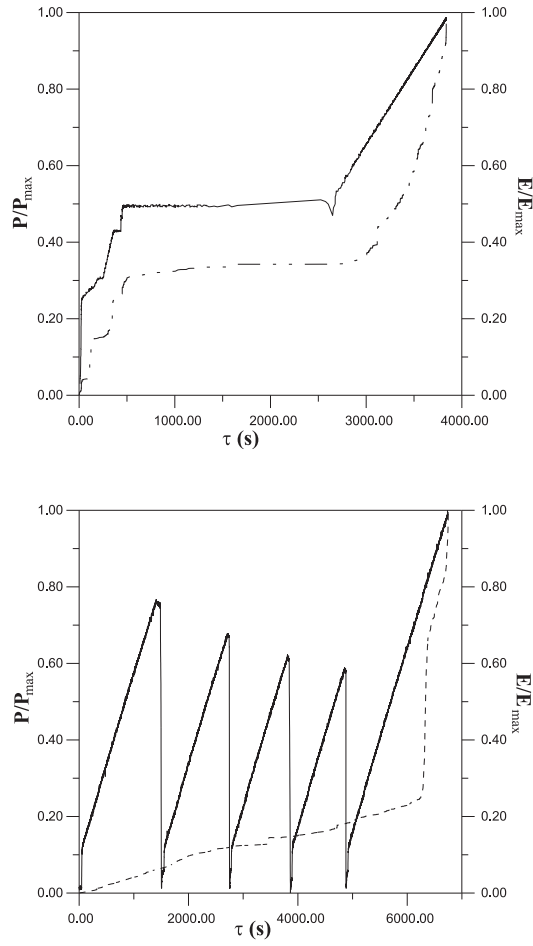


Figure 3: The imposed pressure, normalised at  $P_{\max}$ , and the cumulated energy  $E$ , normalized to  $E_{\max}$ , are plotted as a function of time  $t$ . a) An example of erratic pressure. b) A cyclic pressure.

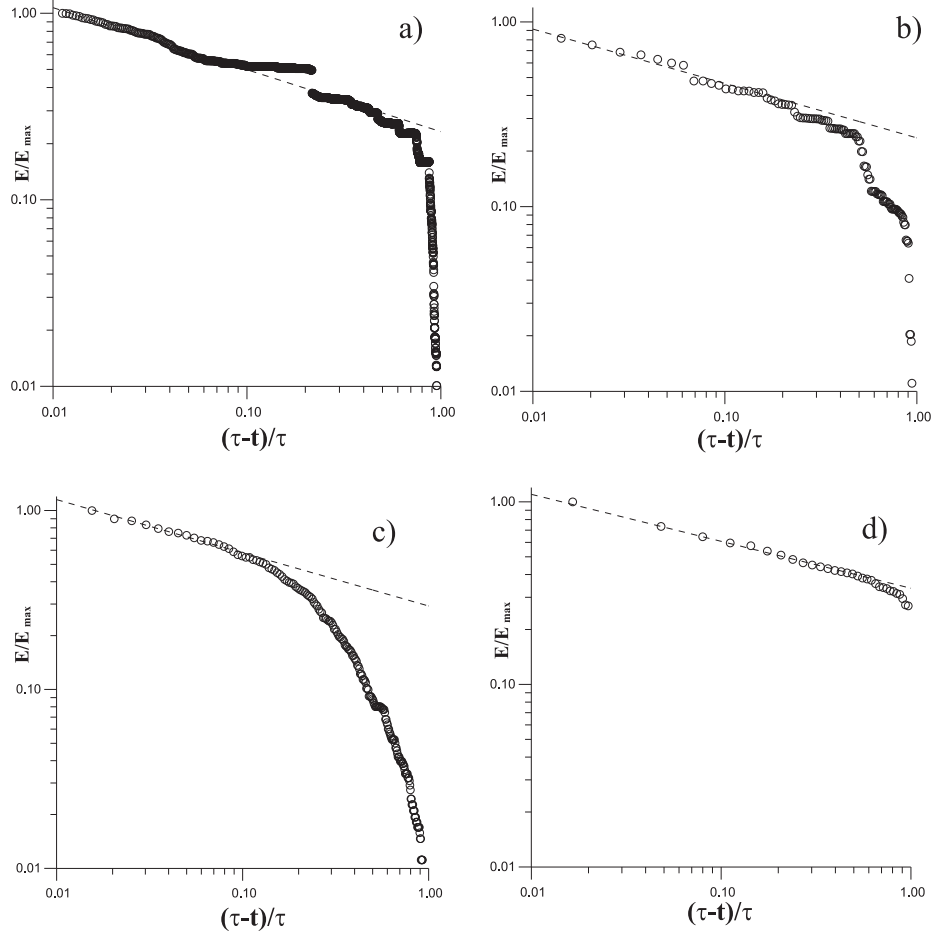


Figure 4: The cumulated energy  $E$ , normalized to  $E_{\max}$ , as a function of the reduced control parameter  $\frac{\tau-t}{\tau}$  at the neighborhood of the fracture point. Figure d) represent the measure taken, at imposed constant rate force, on the tensile machine. The other figures represent measures made on the HPC apparatus at : imposed constant pressure (c), imposed cyclic pressure (a) and imposed erratic pressure (b). The dotted lines are the fit  $E = E_0 \left(\frac{\tau-t}{\tau}\right)^{-\gamma}$ . The exponents found are:  $\gamma = 0.29$  (a),  $\gamma = 0.25$  (b),  $\gamma = 0.29$  (c) and  $\gamma = 0.27$  (d). In the case of a constant pressure rate (on the HPC machine) the same law has been found [24, 23]